Integrative Biology

PAPER

Cite this: *Integr. Biol.*, 2018, **10**, 464

Molecular vibration as a novel explanatory mechanism for the expression of animal colouration†

Ismael Galván, *[a] Javier Cerezo, [b] Alberto Jorge[c] and Kazumasa Wakamatsu [d]

Received 6th June 2018,
Accepted 18th June 2018

DOI: 10.1039/c8ib00100f

rsc.li/integrative-biology

Animal colouration is characterized by the concentration of pigments in integumentary structures and by the nanoscale arrangement of constitutive elements. However, the influence of molecular vibration on colour expression has been overlooked in biology. Molecular vibration occurs in the infrared spectral region, but vibrational and electronic properties can influence each other. Thus, the vibration of pigment molecules may also affect their absorption properties and the resulting colours. We calculated for the first time the relative contribution of molecular vibration (by means of Raman spectroscopy) and concentration (by means of HPLC) of melanin polymers, the most common animal pigments, to generate diversity in plumage colour in 47 species of birds. Vibrational characteristics explained >9 times more variance in colour expression than the concentration of melanins. Additionally, we modelled melanin Raman spectra on the basis of the chemical structure of their constituent monomers and calculated the Huang–Rhys factors for each vibrational mode, which indicate the contribution of these modes to the electronic spectra responsible for the resulting colours. High Huang–Rhys factors frequently coincided with the vibrational modes of melanin monomers. Our results can be explained by the influence of molecular vibration on the absorption properties of melanins. The colour of organisms may thus mainly result from the vibrational properties of their molecules and only residually from their concentration. As a given melanin concentration can give rise to different colours because different structural melanin conformations can present different vibrational characteristics, vibrational effects may favour phenotypic plasticity and thus constitute an important evolutionary force.

Insight, innovation, integration

Using bird plumage colouration and melanins, the most common pigments in animals, as study models, we show that colour phenotypes are mainly explained by the vibrational characteristics of pigment molecules and only residually by the concentration of different chemical forms of pigments as has been considered so far. A given pigment concentration may thus give rise to different colours if vibrational characteristics change, probably because of different conformations of melanin polymers. Computational analyses suggest that our findings may be due to vibrational characteristics affecting the capacity to absorb visible light, which may allow animals to achieve phenotypic plasticity. Therefore, this novel mechanism probably constitutes an important evolutionary force and opens a new field in biology that should now be explored.

Introduction

Visual traits are the most important and widespread mechanisms of animal communication.[1] In many cases, as exemplified by bird plumage colouration, these represent the most diverse phenotypic traits that can be observed in nature, and as a consequence research on visual traits has played a crucial role in the establishment and development of sexual selection and speciation theories.[2] Animals get the optical properties associated to visual traits by two main mechanisms: the use of chemical compounds

[a] *Department of Evolutionary Ecology, Doñana Biological Station, CSIC, 41092 Sevilla, Spain. E-mail: galvan@ebd.csic.es*
[b] *Department of Physical Chemistry, University of Murcia, Campus Espinardo, 30100 Murcia, Spain*
[c] *Laboratory of Non-Destructive Analytical Techniques, National Museum of Natural Sciences, CSIC, 28006 Madrid, Spain*
[d] *Department of Chemistry, Fujita Health University School of Health Sciences, Toyoake, Aichi 470-1192, Japan*

† Electronic supplementary information (ESI) available. See DOI: 10.1039/c8ib00100f

(pigments) and the development of specialized integumentary structures able to generate distinctive optical properties,[3] although pigments and specialized structures often interact. Thus, the colours expressed in the integument of animals are characterized by the pigment or structure that it contains. This characterization is key for understanding the evolution of visual traits, because it provides an indication of the constraints associated to the acquisition of pigments or specialized structures. These constraints, in turn, determine the intensity at which individual animals can express visual traits and thus obtain fitness benefits,[4–6] thus affecting the evolvability of traits.

However, biologists have traditionally overlooked a fundamental concept in physics, which states that molecules exhibit constant movement because of vibrations of their covalent bond network (see, *e.g.* ref. 7). These vibrations can occur at different intensities and following different modes, including synchronous and asynchronous bond stretching, angle bending or dihedral torsions.[8] Molecular vibration produces Raman scattering of light.[9] Although molecules vibrate at frequencies in the infrared (IR) spectral region while the visible absorption spectra of molecules (*i.e.*, colour) derive from the energy states of their constitutive electrons, vibrational and electronic properties of molecules influence each other (*i.e.*, vibronic coupling). Indeed, the broadening of electronic spectral stems from the nuclear dynamics of the solute and the environment.[10] Concretely, in the case of the solute, the vibrational progressions are mainly responsible for the shape of the band, and their extension is related to structural differences between the minima at the initial and final electronic states and on the frequency of the most displaced modes. Therefore, the knowledge of the vibrational pattern is a prerequisite to properly model the nuclear contributions to the lineshape and, moreover, this makes a potential connection between vibrational spectroscopies (*e.g.*, Raman) and the broadening of the final electronic spectra. This means that colour traits are not only the result of changes in the energetic states of electrons in the constitutive molecules of pigments or specialized structures, but they are also tuned by the effect of molecular vibrations.

Thus, in pigments that appear with different structural conformations (*e.g.*, molecular assemblies as in polymers), these will be associated to variation in the frequency, intensity or mode of molecular vibration.[11] However, these structural changes should not necessarily be associated to pigment concentration. If this was the case, pigment molecular vibration would be a better predictor of the optical properties (*i.e.*, colours) than pigment concentration. This possibility, however, has never been contemplated in evolutionary biology. Nevertheless, there is evidence that vibronic coupling predicts the visible absorption spectra of biomolecules, including those of many biological pigments like flavins[12] and carotenoids,[13] and even the perceived colours produced by anthraquinones.[14] If such vibrational effects would be relevant in pigments that are synthesized by animals, this would have deep evolutionary implications, as the genetic and physiological basis of synthesizing pigments with different structural conformations and vibrational characteristics during development may be under selection.

Here we explore this new field in biology to determine the magnitude of the contribution of molecular vibration to explain optical properties of pigments in animal visual traits. Our results show that the vibrational characteristics of pigments are more relevant than their concentration for explaining the observed diversity in animal colouration. Melanins are biopolymers that constitute the most ubiquitous and ancient pigments found in nature[15] and are synthesized by animals in specialized cells called melanocytes,[16] so we use these molecules as study models. Our aim could be achieved as a consequence of recent advances in the study of melanins. First, the slope of the reflectance spectra of feathers and hairs containing melanins has been shown to be a good predictor of the perceived variation in the colours that they generate[17] (see also Experimental). Additionally, recent analyses of Raman scattering have proved that specific signal from the two main chemical forms of melanins (*i.e.*, eumelanin, polymers composed of indole units, and pheomelanins, composed of sulphur-containing heterocycles[18]) can be detected by non-destructive spectroscopic examination of biological tissues.[19–23]

We therefore obtained feather samples from 47 diverse species across the avian phylogeny (12 orders and 30 families), comprising a comprehensive diversity of colours that natural melanins can generate (Table S1 in ESI†). We quantified the expression of colour by analysing the feathers by reflectance spectroscopy and calculating the slope of the reflectance spectra (Fig. 1). Then we determined the vibrational characteristics of melanins contained in the same feathers by non-destructive micro-Raman spectroscopy (Fig. 1 and Table S2 in ESI†), and finally determined the concentration of melanins in the feathers by high-performance liquid chromatography (HPLC) after a chemical degradation of the pigments. Partial least-squares regression (PLSR) analyses[24] allowed us to quantify the relative contribution of melanin vibrational characteristics and of melanin concentration to generate the observed variation in colour expression. To confirm the conclusions obtained from our empirical analyses, we finally conducted simulations of Raman spectra given the chemical structure of melanin monomers and calculated the Huang–Rhys factors for each vibrational mode, which provide an indication of the contribution of these modes to the vibrational broadening of the UV-visible electronic transitions (*i.e.*, resulting colours). Huang–Rhys factors reflect the structural displacement associated to the electronic transition for each normal mode and, consequently, they are directly related to the extent of the progressions of such modes in the vibronic spectra.[25] Large Huang–Rhys factors imply large progressions, and thus determine the involvement of the modes tuning the spectral shape.

Experimental

Sampling

For each species, we obtained two feathers from one bird specimen deposited in the bird collection of the National Museum of Natural Sciences (MNCN, Madrid, Spain; mean

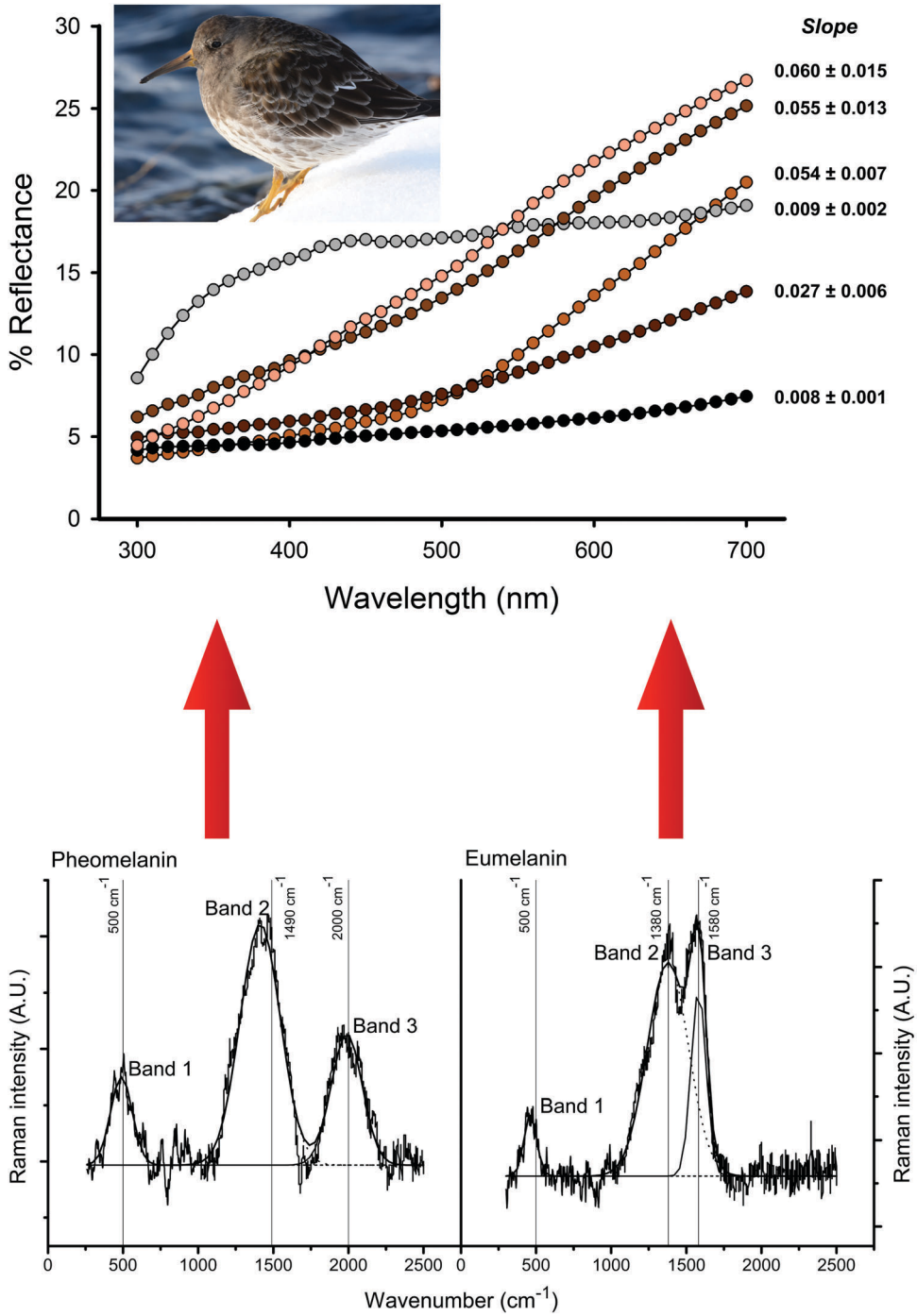

Fig. 1 Upper figure: Mean reflectance spectra of melanin-containing feathers from 47 species of birds, categorized by colour hues as perceived by humans (black, grey, dark brown, dark orange, light brown and light orange). The colour of symbols only serves as an orientation to the resulting hues. Error bars are omitted for clarity. The mean slope ± se of percent reflectance regressed against wavelength is depicted in the right side of the figure. The photograph shows a purple sandpiper *Calidris maritima*, species not included in the study, displaying plumage colouration produced by melanins (credit: Ismael Galván). Only specific colour patches, not combinations of colours, were analyzed in each species. Bottom figure: Raman spectra of pheomelanin and eumelanin from feathers (taken from ref. 20) showing the three diagnostic bands of each pigment and the results of fitting deconvolution functions to the curves. Red arrows depict a causal link between spectral characteristics and reflectance spectra.

specimen age ± se: 56.9 years ± 4.2) or the Icelandic Institute of Natural History (RM, Reykjavic, Iceland; mean specimen age ± se: 60.7 years ± 2.1), excepting feathers from two species (*Sitta europaea* and *Anas strepera*), which were taken from wild birds. Specimens from MNCN and RM did not differ in age (ANOVA: $F_{1,37} = 0.09$, $P = 0.759$). The species were chosen on the basis of homogeneity in the colour patches that were analysed, *i.e.* avoiding complex plumage patterns consisting in differently

perceived colour hues. We avoided iridescent colourations, as these are generated by melanosome morphology and not by melanin chemistry.[26] The number of species was thus chosen on the basis of these criteria while comprising the full palette of colours produced by melanins.[17]

Analysis of colour expression

We measured the colour expression of feathers by reflectance spectrophotometry, using an Ocean Optics (Dunedin, FL, USA) Jaz spectrophotometer (range 220–1000 nm) with UV (deuterium) and visible (tungsten-halogen) lamps and a bifurcated 400 μm fiber optic probe. The fiber optic probe both provided illumination and obtained light reflected from the sample, with a reading area of *ca.* 1 mm^2. Feathers were mounted on a light absorbing foil sheet (Metal Velvet coating, Edmund Optics, Barrington, NJ, USA) to avoid any background reflectance. Measurements were taken at a 90° angle to the sample. All measurements were relative to a diffuse reflectance standard tablet (WS-1, Ocean Optics), and reference measurements were frequently made. An average spectrum of five readings on different points of the target colour patches in feathers was obtained for each bird, removing the probe after each measurement. Only one specific colour patch was measured in each species (Table S1, ESI†). The analyses were made on individual feathers separately, and mean spectra were then calculated. Reflectance curves were obtained by calculating the median of the percent reflectance in 10 nm intervals.

As the reflectance of melanins steadily increases from 300 to 700 nm and shows no spectral peaks,[27] variation in the perceived colour generated by melanins may be given to a large extent by variation in the slope of the reflectance curves. We therefore calculated the slope of percent reflectance regressed against wavelength and used it as a descriptive measurement of melanin-based colour expression. To determine if this measurement actually collects the perceived variation in melanin-based colouration, we assigned the studied species to one of six colour categories that increased with decreasing darkness as perceived by humans (*i.e.* increasing from black to orange). Thus, colour categories and their corresponding values were: black (1), grey (2), dark brown (3), dark orange (4), light brown (5) and light orange (6) (Table S1, ESI†).[17] We therefore regressed slope values against this scale, and found a significant correlation when slope was calculated considering the visible spectral range (400–700 nm) only ($r = 0.64$, $n = 47$, $P < 0.0001$) as well as when near UV wavelengths (300–400 nm) were also considered ($r = 0.66$, $P < 0.0001$). The categories based on the human perception of color are shown here only to illustrate that the measurement of color used in the analyses (slope of percent reflectance regressed against wavelength) collects color variation that might be biologically relevant, as human perception reliably detects variation in the plumage color of birds.[28] Indeed, the correlation between slope and human-based color categories indicates that our measurement of slope reliably explains the perceived variation in melanin-based color phenotypes. The most commonly used parameter to quantify colour expression from melanin reflectance spectra, namely the sum of reflectance values (frequently referred to as brightness[27]) was weakly correlated with the human-based colour categories (300–700 nm: $r = 0.32$, $P = 0.027$; 400–700 nm: $r = 0.39$, $P = 0.006$), as previously reported.[17] This suggests that the slope is a more biologically relevant parameter to quantify variation in reflectance spectra than the sum of reflectance values. Furthemore, PLSR models (see below) did not result in any significant component when brightness instead of slope was considered as the response variable. We therefore calculated the mean slope of the two feathers analysed for each specimen.

Analysis of vibrational characteristics

The same feathers analysed for colour expression were then analysed in a Thermo Fisher DXR confocal dispersive Raman microscope (Thermo Fisher Scientific, Madison, WI, USA) with a point-and-shoot Raman capability of 1 μm spatial resolution and using a near-infrared excitation laser of 780 nm. Laser power was set at 6–8 mW when obtaining pheomelanin spectra, and at 2–3 mW when obtaining eumelanin spectra. The integration time was 5 s for pheomelanin spectra and 3 s for eumelanin spectra, with 8 accumulations for both cases. The single spectra were obtained using a 50× confocal objective and a slit aperture of 25 μm. These conditions produced an average spectral resolution of 2.2–4.4 cm^{-1} in the wavenumber range of 150–2500 cm^{-1}. The average Raman linewidth (FWHH) obtained from four spectra in two bands of polystyrene centered at 1002.30 cm^{-1} and 1603.06 cm^{-1} was 6.2 cm^{-1} and 8.9 cm^{-1}, respectively. The system was operated with Thermo Fisher OMNIC 8.1 software. Calibration and aligning of the spectrograph were checked using pure polystyrene.

The laser beam was focused at different barbs and barbules chosen at random until obtaining five single spectra of pheomelanin and five single spectra of eumelanin for each feather. Thus, every single Raman spectra was categorized as either pheomelanin-based or eumelanin-based. We used the diagnostic bands 1, 2 and 3[20] to assign the Raman spectra to either pheomelanin or eumelanin. Some eumelanin spectra also showed a band around 2000 cm^{-1} coinciding with pheomelanin's band 3[19,20,23], probably as a result of collecting mixed Raman signal from pheomelanin and eumelanin. However, we treated this band as an additional, fourth band for eumelanin in the statistical analyses.

We fitted Voigt deconvolution functions to the mean Raman curves for pheomelanin and eumelanin obtained from the two feathers of each bird specimen, considering the three bands for pheomelanin and eumelanin described above (Fig. 1), and a fourth band for eumelanin when present. From the deconvolution functions, we obtained the spectral position, the intensity, the width at half maximum and the area for each diagnostic Raman band. The analyses of the Raman spectra were made with Thermo Fisher OMNIC 8.1 software. When no Raman signal from pheomelanin or eumelanin was found in any sample, a zero value was assigned to the vibrational characteristics of the corresponding pigment.

Analysis of melanin concentration

The same feathers analysed for colour expression and vibrational characteristics were finally analysed by HPLC, which

allows the detection of specific degradation products of melanins that are specific to the different structural units (monomers) of eumelanins and pheomelanins. In particular, pyrrole-2,3,5-tricarboxylic acid (PTCA) and pyrrole-2,3-dicarboxylic acid (PDCA), which are specific markers of the indole units of eumelanins (5,6-dihydroxyindole-2-carboxylic acid (DHICA) and 5,6-dihydroxyindole (DHI) moieties), and 4-amino-3-hydroxyphenylalanine (4-AHP) and thiazole-2,4,5-tricarboxylic acid (TTCA), which are specific of benzothiazine and benzothiazole pheomelanin moieties, respectively.[29,30] The feathers were first homogenized with Ten-Broeck glass homogenizer at a concentration of 10 mg ml^{-1} water (removing barbs and rachis parts not corresponding to the target colour patch), and then using alkaline H_2O_2 oxidation of eumelanin and pheomelanin to measure PTCA, PDCA and TTCA levels[30] and reductive hydrolysis of pheomelanin with hydriodic acid (HI) to measure 4-AHP levels.[29]

HI reductive hydrolysis products were analysed with an HPLC system consisting of a JASCO 880-PU liquid chromatography, a JASCO C18 column (JASCO Catecholpak; 4.6 × 150 mm; 7 μm particle size) and an EICOM ECD-300 electrochemical detector (Eicom, Kyoto, Japan). The mobile phase was 0.1 M sodium citrate buffer, pH 3.0, containing 1 mM sodium octanesulphonate and 0.1 mM Na_2EDTA : methanol, 98 : 2 (v/v). The electrochemical detector was set at +500 mV *vs.* an Ag/AgCl reference electrode.

H_2O_2 oxidation products were analysed using a Shiseido C18 column (Shiseido Capcell Pak MG; 4.6 × 250 mm; 5 μm particle size; Shiseido Co., Ltd, Tokyo, Japan) and a JASCO UV detector. The mobile phase was 0.1 M potassium phosphate buffer, pH 2.1 : methanol, 99 : 1 (v/v). The absorbance of the eluent was monitored at 269 nm.

Statistical analyses

We calculated the differential contribution of vibrational characteristics (spectral position, intensity, width at half maximum and area of each Raman band) and melanin concentration (PTCA, PDCA, 4-AHP and TTCA levels) (predictor variables) to explain variability in colour expression (slope; response variable) using PLSR models. This is an appropriate statistical technique to analyse the predictive capacity of highly intercorrelated predictor variables,[24] as in the case of vibrational characteristics and markers of melanin concentration.[20,31] PLSR is an extension of multiple regression analysis in which associations are established with components extracted from predictor variables that maximize the explained variance in the response variable. These components are defined as a linear combination of predictor variables, so the original multidimensionality is reduced to a small number of orthogonal components to detect structure in the relationships between predictor variables and between these factors and the response variable. All predictor variables were $\log_{10}$-transformed prior to analyses to achieve normality assumptions. The significance of the extracted PLSR components was determined with two criteria. First, a cross-validation test of the parameter Q_2 was carried out to determine if a component was significant. Then, we tested the significance of the correlation coefficient of the relationship between PLSR scores for the response variable and PLSR component scores, thus determining if the amount of variance explained in the response variable was significant. We also tested the statistical significance of the regression coefficients of the predictors in the PLSR models to determine the degree of correlation between the response variable and these predictors, which was made by bootstrapping using 1000 replications.[31]

Computational methods

To investigate the role of active Raman modes on the UV-visible spectra of melanins we computed the Huang–Rhys factors associated to the lowest energy bright electronic transitions in the most relevant monomers of eumelanin and pheomelanin. In the case of eumelanin, these monomers are DHI and DHICA and their corresponding orthoquinones: 5,6-indolequinone (IQ) and indole-2-carboxylic acid-5,6-quinone (IQCA)[32] (Fig. 3). In the case of pheomelanin, the monomers are a benzothiazine and a benzothiazole[18] (Fig. 3). Simulations were performed evaluating the potential energy surfaces of the monomers at the ground and excited electronic states with Density functional theory methods (DFT) and their TD extension (TDDFT) for the excited states, adopting the Becke, three-parameter, Lee–Yang–Parr (B3LYP) hybrid functional[33] along with the 6-31G(d) basis set. The Gaussian 09 program package[34] was used to carry out the calculations. Raman spectra were obtained at the ground state minimum energy structure. The Huang–Rhys factors account for the geometrical relaxation of the excited states upon excitation, thus requiring the optimization of each electronic state under consideration. The actual factors are then computed using the following equation:

$$S_i = \left(\frac{2\pi\nu_i}{2\hbar}\right)(\Delta Q_i)^2$$

where ν_i are the frequencies associated to the normal modes, $\hbar$ is the Planck constant and ΔQ_i are the normal mode displacements between the equilibrium positions of the ground and excited states, which are related to the geometrical differences through:

$$\Delta Q_i = \sum_{k=1}^{\mathrm{Nat}} m_k^{1/2}\left(L_{xk,i}\Delta x_k + L_{yk,i}\Delta y_k + L_{zk,i}\Delta z_k\right)$$

where m_k are the atomic masses, $L_{\alpha k,i}$ are the elements of the normal mode matrix, and $\Delta\alpha$ ($\alpha = x, y, z$) are the geometrical differences in Cartesian coordinates.

Results

All feathers analysed contained both eumelanin and pheomelanin at different proportions, showing different degrees of variability in the vibrational characteristics (Table S2, ESI†). The PLSR model resulted in a significant component that accounted for 48.6% of variance in the slope of reflectance spectra considering the visible range (400–700 nm), which was significantly correlated with this component ($r = 0.70$, $n = 47$, $P < 0.0001$; Fig. 2). Among the 32 potential

predictors of slope, only the effect of eight of them was statistically significant, seven of these being vibrational characteristics of melanins and only one being an index of melanin concentration (Table 1). The seven significant molecular vibration predictors of colour expression together explained 26.1% of the total variance accounted for by the PLSR model, while the single significant melanin concentration predictor explained 2.8% of that variance, *i.e.* 9.3 times less than molecular vibration predictors. Indeed, the individual effect of the melanin concentration predictor was weaker than the individual effect of any single molecular vibration predictor, as indicated by the absolute value of predictor weights (Table 1). In particular, the vibrational characteristics that predicted colour expression were the spectral position of the three diagnostic Raman bands for pheomelanin, which were positively related to the slope, and the area and Raman intensity of diagnostic bands 2 and 3 for eumelanin, which were negatively related to the slope (Table 1). The spectral position of the three diagnostic Raman bands for pheomelanin were also the vibrational characteristics of pheomelanin with lowest coefficients of variation (Table S2, ESI†). The only melanin concentration index that predicted colour expression was the concentration of the benzothiazole moiety of pheomelanin (TTCA), which was positively related to the slope (Table 1).

We obtained similar results when the slope of reflectance spectra was calculated including near ultraviolet (UV) wavelengths (300–400 nm), which some birds though not humans can perceive,[35] with the exception of the vibrational characteristics of pheomelanin which did not remain as significant predictors (Table 1). The four significant eumelanin vibration predictors of colour expression explained together 18.1% of the total variance accounted for by the PLSR model, while the pheomelanin concentration predictor explained 1.9% of that variance, again representing >9 times less variance than molecular vibration predictors (Table 1).

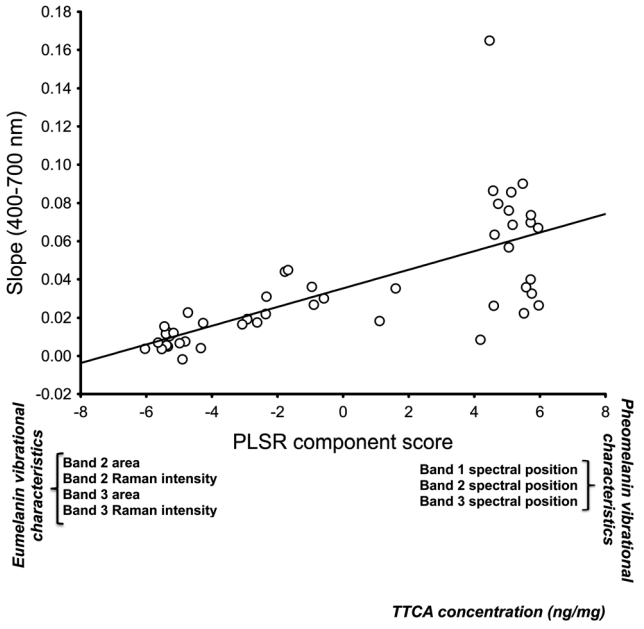

Fig. 2 Relationship between colour expression (measured as the slope of reflectance values regressed against wavelength in the 400–700 nm spectral range) and the scores of a significant component from a partial least-squares regression (PLSR) model testing for the association between colour expression (response variable) and vibrational characteristics and concentration of melanins in feathers (predictor variables). This PLSR component is obtained from a linear combination of the predictor variables (the names of significant predictors below the component indicate which side of the axis increased with increasing values of these predictors) and maximizes the variance that is explained in the response variable. The line is the best-fit line.

Table 1 Results of partial least squares regression (PLSR) models explaining the contribution of vibrational characteristics and concentration of melanins (predictor variables) to generate diversity in plumage colour expression (response variable) in 47 species of birds. Plumage expression is measured as the slope of percent plumage reflectance values regressed against wavelength, excluding (400–700 nm) and including (300–700 nm) the near UV spectral range. Vibrational characteristics refer to the spectral position (*X*), intensity (*Y*), width at half maximum (*W*) and area (*A*) of diagnostic Raman bands 1, 2 and 3 for pheomelanin and Raman bands 1, 2, 3 and 4 for eumelanin. Melanin concentration indexes refer to the concentration (ng mg^{-1} feather) of degradation products that are specific of eumelanin (PTCA and PDCA) and pheomelanin (4-AHP and TTCA). The square of predictor weights indicates the proportion of the total variance accounted for by the PLSR model (indicated at the bottom of the table) that is explained by each predictor variable (*i.e.*, the sum of squared predictor weights equals 1). Asterisks indicate predictors whose regression coefficients are significant at *P*-values of 0.05 (*), 0.01 (**) or 0.001 (***)

	Slope (400–700 nm)		Slope (300–700 nm)	
Predictor	Regression coefficient	Predictor weight	Regression coefficient	Predictor weight
Pheomelanin X1	**0.0038**	**0.169***	0.0028	0.167
Pheomelanin Y1	−0.0034	0.120	−0.0016	0.120
Pheomelanin W1	−0.0073	0.150	−0.0047	0.149
Pheomelanin A1	−0.0006	0.147	0.0006	0.150
Pheomelanin X2	**0.0031**	**0.169***	0.0022	0.167
Pheomelanin Y2	−0.0027	0.145	−0.0036	0.140
Pheomelanin W2	0.0030	0.160	0.0043	0.162
Pheomelanin A2	0.0005	0.163	0.0003	0.163
Pheomelanin X3	**0.0030**	**0.169***	0.0021	0.167
Pheomelanin Y3	−0.0106	0.100	−0.0084	0.089
Pheomelanin W3	−0.0044	0.136	−0.0043	0.133
Pheomelanin A3	−0.0025	0.122	−0.0026	0.112
Eumelanin X1	−0.0014	−0.210	−0.0008	−0.213
Eumelanin Y1	0.0022	−0.164	0.0014	−0.163
Eumelanin W1	−0.0009	−0.199	−0.0028	−0.202
Eumelanin A1	0.0021	−0.167	0.0015	−0.165
Eumelanin X2	−0.0011	−0.210	−0.0006	−0.213
Eumelanin Y2	**−0.0039**	**−0.205****	**−0.0034**	**−0.209***
Eumelanin W2	0.0008	−0.211	0.0005	−0.211
Eumelanin A2	**−0.0009**	**−0.213****	**−0.0007**	**−0.215***
Eumelanin X3	−0.0010	−0.210	−0.0006	−0.213
Eumelanin Y3	**−0.0038**	**−0.208****	**−0.0033**	**−0.211***
Eumelanin W3	0.0011	−0.209	0.0009	−0.210
Eumelanin A3	**−0.0010**	**−0.213*****	**−0.0008**	**−0.216****
Eumelanin X4	−0.0010	−0.210	−0.0006	−0.213
Eumelanin Y4	−0.0021	−0.169	0.0004	−0.167
Eumelanin W4	−0.0012	−0.197	−0.0031	−0.200
Eumelanin A4	−0.0005	−0.191	−0.0003	−0.190
PTCA	−0.0131	−0.204	−0.0147	−0.219
PDCA	−0.0008	−0.115	0.0023	−0.128
4-AHP	−0.0066	0.133	−0.0075	0.116
TTCA	**0.0434**	**0.168****	**0.0293**	**0.139***
% variance explained	48.60		45.25	

Lastly, our simulations showed high Huang–Rhys factors frequently coinciding with the vibrational modes of melanin monomers (Fig. 3). This was particularly evident in one of the two monomers of pheomelanin (*i.e.*, the benzothiazole) (Fig. 3). The presence of these high Huang–Rhys factors indicates that the molecular vibration of melanins can actually affect their UV-visible spectra.

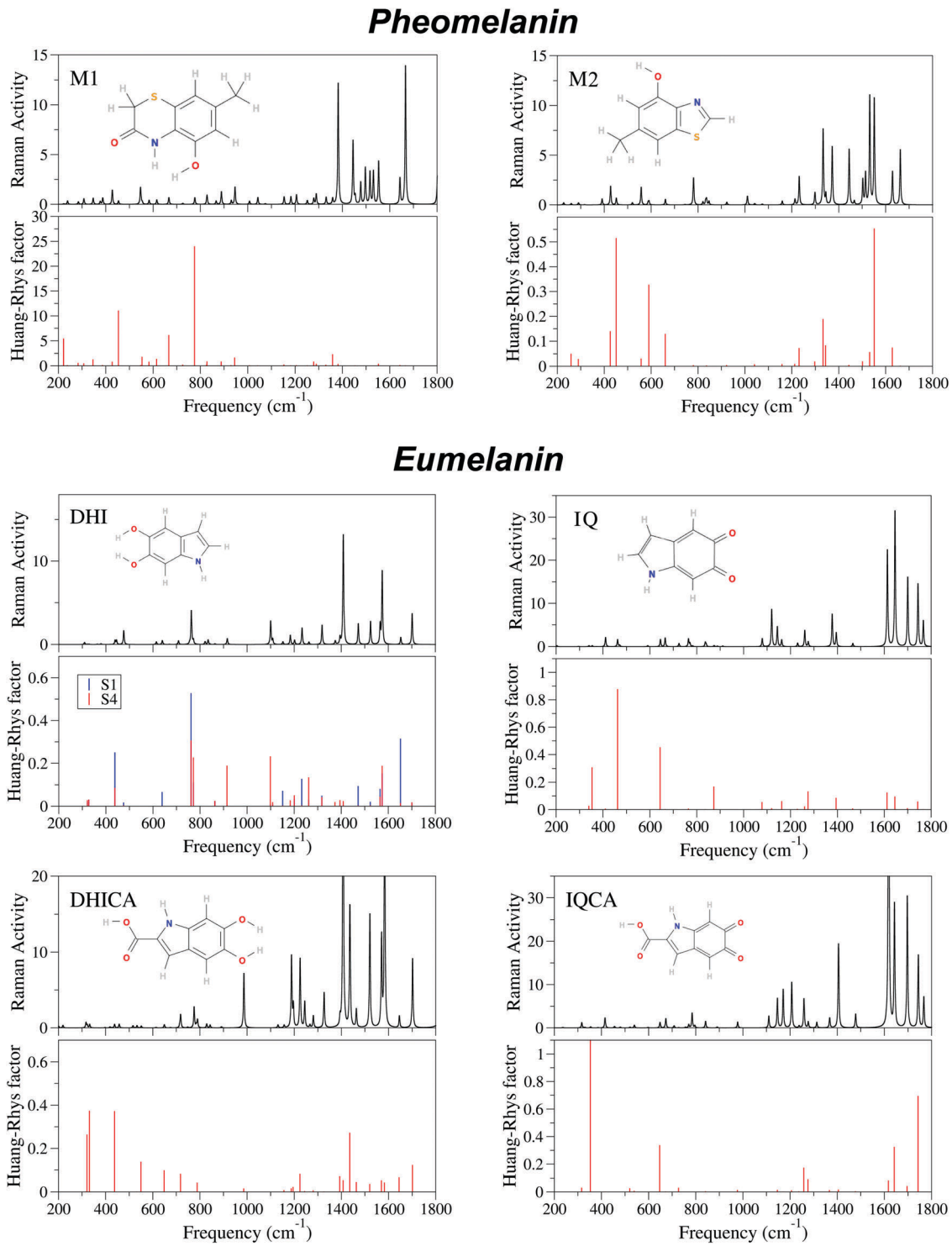

Fig. 3 Computed Raman spectra and Huang–Rhys factors for different monomers constituent of pheomelanin [a benzothiazine (M1) and a benzothiazole (M2)] and eumelanin [5,6-dihydroxyindole (DHI) and 5,6-dihydroxyindole-2-carboxylic acid (DHICA) and their corresponding ortho-quinones: 5,6-indolequinone (IQ) and indole-2-carboxylic acid-5,6-quinone (IQCA)]. Inset are the chemical structures of the monomers. Huang–Rhys factors correspond to the first bright electronic state (S1) of molecules except in DHI, for which the Huang–Rhys factors for the two most intense states (S1 and S4) are shown.

Discussion

These results show that the expression of plumage colouration is mainly explained by vibrational characteristics of melanins contained in feathers, and to a lesser extent by the concentration of these pigments. Vibrational and electronic interactions in molecules are known to influence each other (vibronic coupling), and thus molecular vibration characteristics can affect electric properties and hence visible absorption spectra.[12,13] In fact, vibronic coupling has theoretically been demonstrated to predict the colours produced by the melanin-related pigments termed anthraquinones.[14] This may explain the colour predictive capacity of the vibrational characteristics of melanins.

In order to obtain a preliminar validation of a possible causal link between the vibrational features of Raman spectra and the resulting colours, we have used computational simulations of the Raman spectra and the Huang–Rhys factors for each vibrational mode associated to the first bright electronic transition of the main monomers of eumelanin and pheomelanin. Huang–Rhys factors indicate which modes will be most displaced between ground and excited state minimum structures and thus contribute to the vibrational broadening of the UV-visible electronic transitions.[25] Interestingly, our results show that, in some monomers, the active Raman modes related to the diagnostic bands 1 and 2 used in our statistical analyses are also characterised by large Huang–Rhys factors. This preliminar investigation opens a route to explain the relationship between the vibrational (Raman) spectra of the pigments and their electronic spectra (*i.e.*, their colour).

The out-of-plane deformation and stretching of hexagonal aromatic rings in the pheomelanin polymer gives rise to the diagnostic Raman bands 1 and 2 of this pigment, respectively, while the vibrational characteristics that lead to pheomelanin's band 3 are still unknown.[19,23] Our findings indicate that the spectral shift of these three diagnostic bands makes feathers produce lighter colour hues, *i.e.* reflectance spectra with higher slopes. On the other hand, the stretching of hexagonal rings and three of the six C–C bonds within the rings gives rise to eumelanin's Raman bands 2 and 3, respectively,[19,36] which produce darker hues as their area and intensity increase.

Therefore, these findings represent a new view of the visual phenotype of organisms. This study shows that the vibrational characteristics of biomolecules are not only powerful diagnostic features that allow their identification,[37,38] but they also affect the appearance of organisms by affecting visible optical properties. Interestingly, the vibrational characteristics of pheomelanin that predicted plumage colour expression (*i.e.*, the frequency of the stretching vibration of hexagonal aromatic rings) were also those with the lowest coefficients of variation for this pigment. This stresses the magnitude of the effect of molecular vibration on colour expression, as small changes in pheomelanin vibration lead to perceptible changes in plumage colouration.

This is the first evidence that the same pigment concentration can be associated with different vibrational characteristics and produce different colour phenotypes in animals. At this stage, we can only envision the evolutionary implications that this should have, but these may be relevant from the perspective of both proximate and ultimate mechanisms. From the perspective of proximal mechanisms, the influence of vibrational characteristics on the electronic properties of molecules includes changes in electron delocalization,[39–41] which in turn affects the capacity of biomolecules to stabilize (*i.e.* scavenge) free radicals.[42] This is particularly relevant for colour phenotypes produced by melanins, as significant amounts of cytotoxic species, including reactive oxygen species (ROS) such as superoxide and hydrogen peroxide, are formed in melanocytes during the final stages of eumelanin synthesis[43,44] and also in already formed pheomelanins exposed to energetic radiation.[45] Thus, certain colour phenotypes may be associated to certain vibrational characteristics of melanins that would make these molecules especially prone to free radical-mediated cytotoxicity and cellular damage. These possibilities have recently been tested in the chicken, resulting in certain vibrational characteristics of pheomelanin being associated with mitochondrial ROS production in melanocytes and systemic oxidative stress and damage.[31]

From the perspective of the ultimate causes, our study points to an unsuspected potential source of evolutionary change. If the same pigment concentration can give rise to different colour phenotypes through variation in the pigment vibrational characteristics (regardless this effect derives or not from changes in the assembly of pigment components), then this may facilitate creating novel colour phenotypes. As animal colour traits often evolve under sexual selection and influence the degree of isolation of incipient species,[46] it is likely that the vibrational characteristics of pigments affect the process of speciation. This new perspective should also be explored by future studies. In particular, it should be investigated if the relative contribution of vibrational characteristics and pigment concentration to colour expression varies among taxa. If the contribution of vibrational characteristics was higher in some groups than in others, that would lead to an increased phenotypic plasticity in the former. This may favour higher speciation rates or a greater capacity to explode a higher diversity of ecological niches in those groups.[47]

Conflicts of interest

We declare no conflicts of interest.

Acknowledgements

Two anonymous reviewers commented on the manuscript. We thank Josefina Barreiro and Ólafur K. Nielsen their kind collaboration with sampling at the bird collections of the National Museum of Natural Sciences (MNCN, Madrid) and the Icelandic Institute of Natural History (Reykjavic, Iceland), respectively. Rafael Márquez helped with the spectrophotometric analyses of feathers. We acknowledge funding from Fundación BBVA ('Convocatoria 2015 de ayudas Fundación BBVA a investigadores y creadores culturales', reference IN[15]CMA_CMA_1422) to IG. IG is also supported by a Ramón

y Cajal Fellowship (RYC-2012-10237) and the project CGL2015-67796-P from the Spanish Ministry of Economy, Industry and Competitiveness (MINECO). JC acknowledges a fellowship provided by ''Fundación Séneca – Agencia de Ciencia y Tecnología de la Región de Murcia'' through the ''Saavedra-Fajardo'' program (20028/SF/16).

References

1 *The Evolution of Animal Communication*, ed. W. A. Searcy and S. Nowicki, Princeton University Press, New Jersey, NJ, 2005.
2 J. Dale, C. J. Dey, K. Delhey, B. Kempenaers and M. Valcu, The effects of life history and sexual selection on male and female plumage colouration, *Nature*, 2015, **527**, 367–370.
3 *Bird Coloration, Volume 1: Mechanisms and Measurement*, ed. G. E. Hill and K. J. McGraw, Harvard University Press, Cambridge, MS, 2006.
4 R. Olendorf, F. H. Rodd, D. Punzalan, A. E. Houde, C. Hurt, D. N. Reznick and K. A. Hughes, Frequency-dependent survival in natural guppy populations, *Nature*, 2006, **441**, 633–636.
5 G. Pérez i de Lanuza, P. Carazo and E. Font, Colours of quality: structural (but not pigment) coloration informs about male quality in a polychromatic lizard, *Anim. Behav.*, 2014, **90**, 73–81.
6 I. Galván, K. Wakamatsu, P. R. Camarero, R. Mateo and C. Alonso-Alvarez, Low-quality birds do not display high-quality signals: the cysteine-pheomelanin mechanism of honesty, *Evolution*, 2015, **69**, 26–38.
7 *Handbook of Biophotonics, Volume 1: Basics and Techniques*, ed. J. Popp, V. V. Tuchin, A. Chiou and S. H. Heinemann, Wiley-VCH, Weinheim, 2011.
8 *Molecular Vibrations: the Theory of Infrared and Raman Vibrational Spectra*, ed. E. B. Wilson Jr., J. C. Decius and P. C. Cross, McGraw-Hill, New York, NY, 1955.
9 C. V. Raman and K. S. Krishnan, A new type of secondary radiation, *Nature*, 1928, **121**, 501–502.
10 *Computational Strategies for Spectroscopy: from Small Molecules to Nano Systems*, ed. V. Barone, John Wiley & Sons, Inc., Hoboken, NJ, 2011.
11 I. Galván, C. Araujo-Andrade, M. Marro, P. Loza-Alvarez and K. Wakamatsu, Raman spectroscopy quantification of eumelanin subunits in natural unaltered pigments, *Pigm. Cell Melanoma Res.*, 2018, DOI: 10.1111/pcmr.12707.
12 Y. J. Ai, G. Tian, R. Z. Liao, Q. Zhang, W. H. Fang and Y. Luo, Intrinsic property of flavin mononucleotide controls its optical spectra in three redox states, *ChemPhysChem*, 2011, **12**, 2899–2902.
13 J. Cerezo, J. Zúñiga, A. Requena, F. J. Ávila Ferrer and F. Santoro, Harmonic models in cartesian and internal coordinates to simulate the absorption spectra of carotenoids at finite temperatures, *J. Chem. Theory Comput.*, 2013, **9**, 4947–4958.
14 D. Jacquemin, E. Brémond, I. Ciofini and C. Adamo, Impact of vibronic couplings on perceived colors: two anthraquinones as a working example, *J. Phys. Chem. Lett.*, 2012, **3**, 468–471.
15 F. Zhang, S. L. Kearns, P. J. Orr, M. J. Benton, Z. Zhou, D. Johnson, X. Xu and X. Wang, Fossilized melanosomes and the colour of Cretaceous dinosaurs and birds, *Nature*, 2010, **463**, 1075–1078.
16 S. J. Lin, J. Foley, T. X. Jiang, C. Y. Yeh, P. Wu, A. Foley, C. M. Yen, Y. C. Huang, H. C. Cheng and C. F. Chen, *et al.*, Topology of feather melanocyte progenitor niche allows complex pigment patterns to emerge, *Science*, 2013, **340**, 1442–1445.
17 I. Galván and K. Wakamatsu, Color measurement of the animal integument predicts the content of specific melanin forms, *RSC Adv.*, 2016, **6**, 79135–79142.
18 S. Ito and K. Wakamatsu, Chemistry of mixed melanogenesis: pivotal roles of dopaquinone, *Photochem. Photobiol.*, 2008, **84**, 582–592.
19 I. Galván, A. Jorge, F. Solano and K. Wakamatsu, Vibrational characterization of pheomelanin and trichochrome F by Raman spectroscopy, *Spectrochim. Acta, Part A*, 2013, **110**, 55–59.
20 I. Galván, A. Jorge, K. Ito, K. Tabuchi, F. Solano and K. Wakamatsu, Raman spectroscopy as a non-invasive technique for the quantification of melanins in feathers and hairs, *Pigm. Cell Melanoma Res.*, 2013, **26**, 917–923.
21 I. Galván and A. Jorge, Dispersive Raman spectroscopy allows the identification and quantification of melanin types, *Ecol. Evol.*, 2015, **5**, 1425–1431.
22 A. Jorge, C. Polidori and J. L. Nieves-Aldrey, Pheomelanin in the secondary sexual characters of male parasitoid wasps (Hymenoptera: Pteromalidae), *Arthropod Struct. Dev.*, 2016, **45**, 311–319.
23 H. Wang, S. Osseiran, V. Igras, A. J. Nichols, E. M. Roider, J. Pruessner, H. Tsao, D. E. Fisher and C. L. Evans, *In vivo* coherent Raman imaging of the melanomagenesis-associated pigment pheomelanin, *Sci. Rep.*, 2016, **6**, 37986.
24 L. M. Carrascal, I. Galván and O. Gordo, Partial least squares regression as an alternative to current regression methods used in ecology, *Oikos*, 2009, **118**, 681–690.
25 K. Huang and A. Rhys, Theory of light absorption and non-radiative transitions in F-centres, *Proc. R. Soc. London, Ser. A*, 1950, **204**, 406–423.
26 C. M. Eliason, P. P. Bitton and M. D. Shawkey, How hollow melanosomes affect iridescent colour production in birds, *Proc. R. Soc. London, Ser. B*, 2013, **280**, 20131505.
27 K. J. McGraw, R. J. Safran and K. Wakamatsu, How feather colour reflects its melanin content, *Funct. Ecol.*, 2005, **19**, 816–821.
28 Z. T. Bergeron and R. C. Fuller, Using human vision to detect variation in avian coloration: how bad is it?, *Am. Nat.*, 2018, **191**, 269–276.
29 K. Wakamatsu, S. Ito and J. L. Rees, The usefulness of 4-amino-3-hydroxyphenylalanine as a specific marker of pheomelanin, *Pigm. Cell Res.*, 2002, **15**, 225–232.
30 S. Ito, Y. Nakanishi, R. K. Valenzuela, M. H. Brilliant, L. Kolbe and K. Wakamatsu, Usefulness of alkaline

hydrogen peroxide oxidation to analyze eumelanin and pheomelanin in various tissue samples: application to chemical analysis of human hair melanins, *Pigm. Cell Melanoma Res.*, 2011, **24**, 605–613.
31 I. Galván, A. Jorge and M. García-Gil, Pheomelanin molecular vibration is associated with mitochondrial ROS production in melanocytes and systemic oxidative stress and damage, *Integr. Biol.*, 2017, **9**, 751–761.
32 M. d'Ischia, A. Napolitano, A. Pezzella, P. Meredith and T. Sarna, Chemical and structural diversity in eumelanins: unexplored bio-optoelectronic materials, *Angew. Chem., Int. Ed.*, 2009, **48**, 3914–3921.
33 A. D. Becke, A new mixing of Hartree–Fock and local density-functional theories, *J. Chem. Phys.*, 1993, **98**, 1372–1377.
34 M. J. Frisch, G. W. Trucks, H. B. Schlegel, G. E. Scuseria, M. A. Robb, J. R. Cheeseman, G. Scalmani, V. Barone, G. A. Petersson and H. Nakatsuji, *et al.*, *Gaussian 09, Revision A.02*, Gaussian, Inc., Wallingford, CT, 2016.
35 M. D. Eaton and S. M. Lanyon, The ubiquity of avian ultraviolet plumage reflectance, *Proc. R. Soc. London, Ser. B*, 2003, **270**, 1721–1726.
36 Z. Huang, H. Lui, X. K. Chen, A. Alajlan, D. I. McLean and H. Zeng, Raman spectroscopy of *in vivo* cutaneous melanin, *J. Biomed. Opt.*, 2004, **9**, 1198–1205.
37 S. Dochow, C. Krafft, U. Neugebauer, T. Bocklitz, T. Henkel, G. Mayer, J. Albert and J. Popp, Tumour cell identification by means of Raman spectroscopy in combination with optical traps and microfluidic environments, *Lab Chip*, 2011, **11**, 1484–1490.
38 S. Stöckel, S. Meisel, M. Elschner, P. Rösch and J. Popp, Raman spectroscopic detection of anthrax endospores in powder samples, *Angew. Chem., Int. Ed.*, 2012, **51**, 5339–5342.
39 J. C. Bart and C. H. MacGillavry, The crystal and molecular structure of canthaxanthin, *Acta Crystallogr., Sect. B: Struct. Crystallogr. Cryst. Chem.*, 1968, **24**, 1587–1606.
40 P. Cysewski, Influence of thermal vibrations on aromaticity of benzene, *Phys. Chem. Chem. Phys.*, 2011, **13**, 12998–13008.
41 D. Venkateshvaran, M. Nikolka, A. Sadhanala, V. Lemaur, M. Zelazny, M. Kepa, M. Hurhangee, A. J. Kronemeijer, V. Pecunia and I. Nasrallah, *et al.*, Approaching disorder-free transport in high-mobility conjugated polymers, *Nature*, 2014, **515**, 384–388.
42 E. Heim, A. R. Tagliaferro and D. J. Bobilya, Flavonoid antioxidants: chemistry, metabolism and structure-activity relationships, *J. Nutr. Biochem.*, 2002, **13**, 572–584.
43 K. Urabe, P. Aroca, K. Tsukamoto, D. Mascagna, A. Palumbo, G. Prota and V. J. Hearing, The inherent cytotoxicity of melanin precursors: a revision, *Biochim. Biophys. Acta*, 1994, **1221**, 272–278.
44 S. Jiang, X. M. Liu, X. Dai, Q. Zhou, T. C. Lei, F. Beermann, K. Wakamatsu and S. Z. Xu, Regulation of DHICA-mediated antioxidation by dopachrome tautomerase: implication for skin photoprotection against UVA radiation, *Free Radical Biol. Med.*, 2010, **48**, 1144–1151.
45 S. Takeuchi, W. Zhang, K. Wakamatsu, S. Ito, V. J. Hearing, K. H. Kraemer and D. E. Brash, Melanin acts as a potent UVB photosensitizer to cause an atypical mode of cell death in murine skin, *Proc. Natl. Acad. Sci. U. S. A.*, 2004, **101**, 15076–15081.
46 R. J. Rundell and T. D. Price, Adaptive radiation, nonadaptive radiation, ecological speciation and nonecological speciation, *Trends Ecol. Evol.*, 2009, **24**, 394–399.
47 D. W. Pfennig, M. A. Wund, E. C. Snell-Rood, T. Cruickshank, C. D. Schlichting and A. P. Moczek, Phenotypic plasticity's impacts on diversification and speciation, *Trends Ecol. Evol.*, 2010, **25**, 459–467.